



17th International Conference on Greenhouse Gas Control Technologies, GHGT-17

20<sup>th</sup>-24<sup>th</sup> October 2024 Calgary, Canada

## Techno-economic analysis of CO<sub>2</sub> conditioning and transport systems for offshore shipping

Zhengyang Wang, Richard T.J. Porter, Fengyuan Zhang, Haroun Mahgerefteh\*

*Department of Chemical Engineering, University College London, London WC1E 7JE, United Kingdom*

---

### Abstract

Among available modes for transport of captured CO<sub>2</sub>, pressurised pipelines are generally preferred for long distances and attract the most attention. However, limitations such as the high capital expenditure and implementation time have introduced more focus on the emerging marine transportation of CO<sub>2</sub> especially for offshore transport. This more flexible mode of CO<sub>2</sub> transport requires the liquefaction of CO<sub>2</sub> before shipping. This study investigates liquefaction systems for CO<sub>2</sub> ship transport with different feed streams representative of three different types of capture routes (pre-combustion, post-combustion, and oxyfuel) and four industries (cement plant, iron and steel industry, power plant, and refinery) at delivery pressure 7 bar and 15 bar. The methodology results in various liquefaction routes configured using Aspen Plus process simulations, showing that the purities of CO<sub>2</sub> products reach 99% after the liquefaction process in all the cases. The refinery case at the 15 bar delivery pressure presents the lowest levelised cost of \$16.01/tCO<sub>2</sub>.

*Keywords:* Process simulation, techno-economic analysis, CO<sub>2</sub> shipping, liquefaction

---

### 1. Introduction

Climate change is an imminent and pressing global issue that is commonly associated with excessive carbon dioxide (CO<sub>2</sub>) emissions from fossil fuels. Due to the excess of CO<sub>2</sub> in the atmosphere, the greenhouse effect is amplified, increasing the earth's temperature and contributing to global warming. The rapid increase in CO<sub>2</sub> levels is mainly due to human activities and emissions from industries. According to the International Energy Agency [1], the majority of CO<sub>2</sub> emissions originate from industry (28%), electricity (26%), transportation (23%), and other sources. Therefore, it is vital to mitigate climate change and achieve the target emission rates set by The Paris Agreement [2]. The fundamental goal behind this agreement is to limit the rise in global temperature to 2°C and further reduce it to 1.5°C by reducing greenhouse gas emissions. It is international scientific consensus that global net human-caused emissions of CO<sub>2</sub> need to fall by about 45% from 2010 levels by 2030, reaching net zero around 2050 [3]. Carbon Capture and Storage (CCS) technology is considered one of the effective strategies to mitigate climate change in the short term [4].

CCS technology is a combination of CO<sub>2</sub> separating, transporting, and storing CO<sub>2</sub> underground. It presents one of the leading technologies for the large-scale decarbonisation of the global energy system and can be applied to power

---

\* Corresponding author. Email address: h.mahgerefteh@ucl.ac.uk

plants, the iron and steel industry, as well as the high CO<sub>2</sub>-emitting cement production plants [6-9]. Whereas CCS technology has been developed recently to aggregate CO<sub>2</sub> captured at different facilities, one of the major barriers to the wide deployment of CCS is given by the deployment of large-scale CO<sub>2</sub> transportation connecting sources and sinks. More attention should be paid to the transport step and to the analysis of the cost of supply chains.

Among available modes of transport, pressurised pipelines are generally preferred for long distances and, hence the focus of most attention. However, limitations such as the high capital expenditure and implementation time introduce more focus on the emerging marine transportation of CO<sub>2</sub>, especially during offshore transport. This more flexible mode of CO<sub>2</sub> transport requires the liquefaction of CO<sub>2</sub> before being shipped, as shown in Fig. 1. However, the liquefaction process demands large amounts of energy due to the massive volume of CO<sub>2</sub> needed to be liquified. Moreover, given the impact of impurities on CO<sub>2</sub> transportation, many studies focus on purifying the CO<sub>2</sub> stream economically [10-16]. The liquefaction procedure prior to transportation can reduce the levels of impurities to a certain extent and can also be coupled with other purification processes on an as-needed basis.

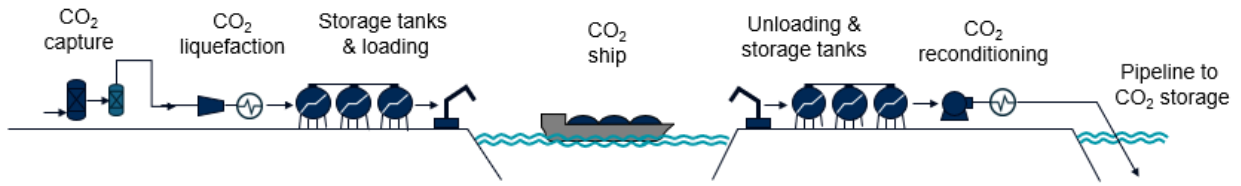


Fig. 1. CCS chain with shipping between two harbours.

This study focuses on identifying cost-effective routes for the CO<sub>2</sub> liquefaction process in shipping transportation. A parametric study on liquefaction and delivery pressures is also carried out by comparing the liquefaction costs. Furthermore, the impact of impurities in the CO<sub>2</sub> stream on liquefaction costs is also investigated by comparing simulations of CO<sub>2</sub> liquefaction between a pure CO<sub>2</sub> stream and multiple scenarios of CO<sub>2</sub> streams with different compositions of impurities from different capture sources. The techno-economic analysis will be done as a basis for gauging the performance of the liquefaction system throughout the simulations done by using Aspen Plus in the process design of the liquefaction system and in investigating the impacts of impurities on the process.

## 2. Methodology

### 2.1. Flowsheet of the liquefaction system

The flowsheet of the liquefaction process is shown in Fig. 2. The FEED stream containing water as an impurity must first pass through a dehydration unit equipped with molecular sieves. At the compression part, the CO<sub>2</sub> feed stream goes through a 3-stage compression process to be compressed to the liquefaction pressure of 19.7 bar (stream 7). Then, stream 7 is mixed with the recycled stream 17 at B7. Some condensable impurities like water are separated at B8. The liquefaction process is done at heat exchanger B9, where CO<sub>2</sub>-rich stream 10 is liquefied to stream 11 and then some non-condensable impurities are separated at B22, flowing out of the process in stream IMPURITY. The pressure of the CO<sub>2</sub> product drops at B23 to the delivery pressure and after the separate B24, the liquefied CO<sub>2</sub> is in stream LIQUID for delivery. Ammonia is used as the refrigerant in the refrigeration part. From stream 18 to stream 24, the ammonia goes through a 3-stage compression process, reaching 14 bar at stream 24. Then, the pressure and temperature drop through the Joule-Thompson effect reaching around -25 °C at stream 32 to liquefy CO<sub>2</sub>. In the recycle part, the vapour fraction of CO<sub>2</sub> from B24 is compressed to 19.7 bar again to mix with the compressed feed stream 7. Fig. 3 is the CO<sub>2</sub> phase diagram with the CO<sub>2</sub> state of the key streams of the flowsheet.

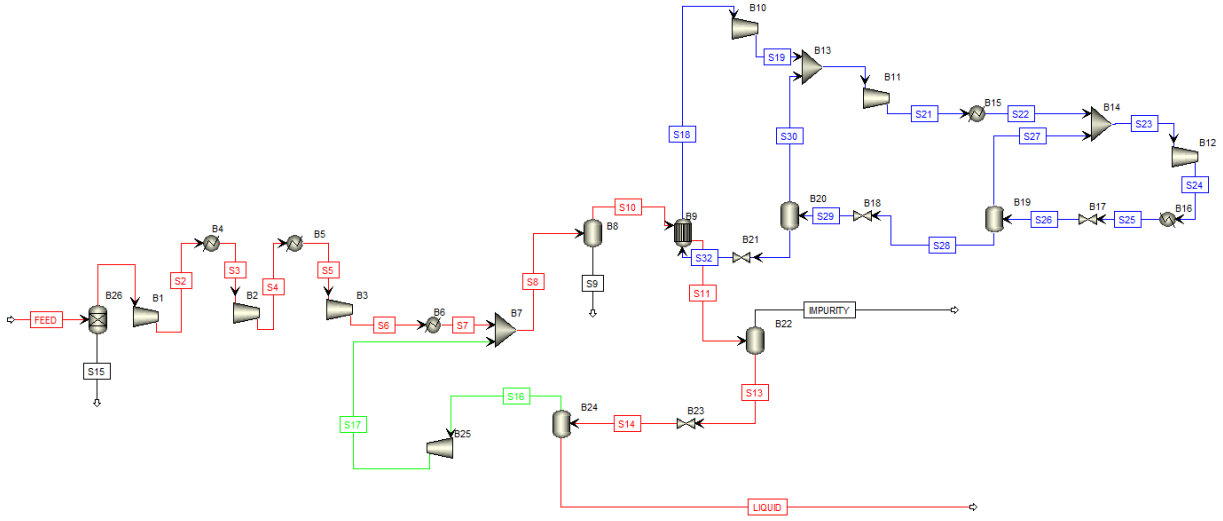


Fig. 2. Flowsheet of the liquefaction process. Red line:  $\text{CO}_2$  main stream; Blue line: refrigeration stream; Green line:  $\text{CO}_2$  recycle stream.

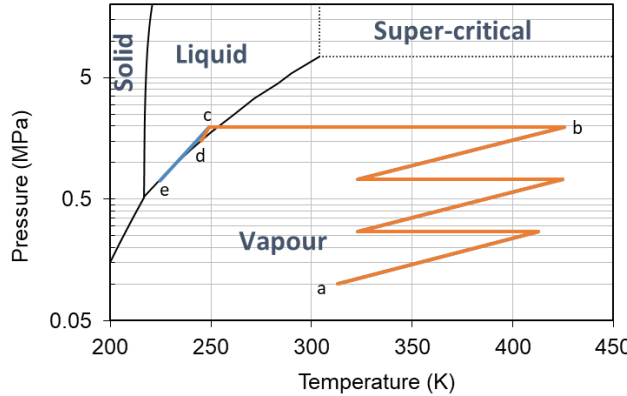


Fig. 3.  $\text{CO}_2$  phase diagram with the  $\text{CO}_2$  state of the key streams of the flowsheet. Orange line: pure  $\text{CO}_2$  case whose delivery pressure is at 15 bar; Blue line: pure  $\text{CO}_2$  case whose delivery pressure is at 7 bar. Point a–b: 3-stage compression process; b–c: liquefaction process; c–d and c–e: pressure drops to delivery pressure.

## 2.2. $\text{CO}_2$ feed stream

Three impurity cases using three different capture methods are selected as feed streams: (1) Case 1 using pre-combustion method [17]; (2) Case 2 using post-combustion method [18]; (3) Case 3 using Oxyfuel method [19]. The composition of each case is presented below in Table 2.1.

Another four impurity cases from different industries are selected as feed streams based on previous studies: (1) Case 4 from a cement plant [20]; (2) Case 5 from the iron and steel industry [21]; (3) Case 6 from a power plant [22]; (4) Case 7 from a refinery [23]. The composition of each case is presented below in Table 2.2. Case 8 is the pure  $\text{CO}_2$  stream for comparison purposes.

Table 2.1. Composition of the feed stream in Cases 1-3.

| Capture method         | Pre-combustion | Post-combustion | Oxyfuel |
|------------------------|----------------|-----------------|---------|
| CO <sub>2</sub> [%]    | 98.42          | 95.87           | 97.40   |
| N <sub>2</sub> [%]     | 0.44           | 0.02            | 1.50    |
| Ar [%]                 | 0.09           | -               | -       |
| H <sub>2</sub> O [%]   | -              | 4.11            | -       |
| O <sub>2</sub> [%]     | -              | 0.001           | 1.10    |
| CH <sub>3</sub> OH [%] | 0.57           | -               | -       |
| H <sub>2</sub> [%]     | 0.45           | -               | -       |
| CO [%]                 | 0.03           | -               | -       |
| H <sub>2</sub> S [%]   | 0.0005         | -               | -       |
| SO <sub>2</sub> [%]    | -              | 0.001           | -       |

Table 2.2. Composition of the feed stream in Cases 4-7.

| Industries           | Cement | Iron and steel | Power plant | Refinery |
|----------------------|--------|----------------|-------------|----------|
| CO <sub>2</sub> [%]  | 96.86  | 98.79          | 95.02       | 95.0     |
| N <sub>2</sub> [%]   | 0.11   | 0.09           | 0.40        | 0.2      |
| H <sub>2</sub> O [%] | 3.00   | 1.08           | 1.22        | 4.8      |
| O <sub>2</sub> [%]   | 0.03   | 0.04           | 3.36        | -        |

### 2.3. Delivery Pressure

The delivery pressures can have an impact on the purity of the CO<sub>2</sub> to be transported. 7 bar and 15 bar, referred to as low pressure and medium pressure, are selected as delivery pressure in this study.

### 2.4. Cost calculation methodology

Since all the simulations are done by Aspen Plus, the Aspen Process Economic Analyzer is used to obtain the CAPEX and OPEX. The CAPEX includes equipment purchase, labour, installation and material costs. The OPEX is calculated based on the hot and cold utility in the process. The tool estimates the CAPEX and OPEX in each simulation and these values will be the basis for the overall cost calculation.

The levelised cost is considered as the performance indicator, where the unit of the value is dollars per ton of liquefied CO<sub>2</sub> for delivery. The equation to calculate the levelised cost is shown below:

$$\text{Levelised cost} = \frac{\frac{\text{CAPEX}}{\text{Plant lifetime}} + \text{OPEX}}{\text{Annual liquefied CO}_2 \text{ produced}} \quad (1)$$

Where the plant lifetime is assumed to be 25 years for all the industries and the plant is assumed to run non-stop for 25 years. The annual liquefied CO<sub>2</sub> produced can be calculated from the flow rates of the CO<sub>2</sub> product stream.

## 3. Results and discussions

### 3.1. CO<sub>2</sub> product composition

The composition of the CO<sub>2</sub> product streams of Cases 1-3 and Case 8 for both delivery pressures is recorded from Aspen Plus stream results, as shown in Table 3.1. The composition of the feed stream of each case is added in Fig. 3

and Fig. 4 to show the difference in the composition of the CO<sub>2</sub> and impurities between the feed stream and the product stream.

Table 3.1. Composition of CO<sub>2</sub> production streams in Cases 1-3 and Case 8.

|                        | Pre-7 | Pre-15 | Post-7 | Post-15 | Oxy-7 | Oxy-15 | Pure-7 | Pure-15 |
|------------------------|-------|--------|--------|---------|-------|--------|--------|---------|
| CO <sub>2</sub> [%]    | 99.35 | 99.23  | 99.98  | 99.98   | 99.92 | 99.75  | 100    | 100     |
| N <sub>2</sub> [%]     | 0.01  | 0.10   | 0.02   | 0.02    | 0.02  | 0.08   | -      | -       |
| Ar [%]                 | 0.01  | 0.04   | -      | -       | -     | -      | -      | -       |
| H <sub>2</sub> O [%]   | -     | -      | 0.00   | 0.00    | -     | -      | -      | -       |
| O <sub>2</sub> [%]     | -     | -      | 0.001  | 0.001   | 0.06  | 0.17   | -      | -       |
| CH <sub>3</sub> OH [%] | 0.63  | 0.62   | -      | -       | -     | -      | -      | -       |
| H <sub>2</sub> [%]     | 0.00  | 0.01   | -      | -       | -     | -      | -      | -       |
| CO [%]                 | 0.00  | 0.00   | -      | -       | -     | -      | -      | -       |
| H <sub>2</sub> S [%]   | 0.00  | 0.00   | -      | -       | -     | -      | -      | -       |
| SO <sub>2</sub> [%]    | -     | -      | 0.001  | 0.001   | -     | -      | -      | -       |

Fig. 4 shows the CO<sub>2</sub> composition of the feed stream and product stream in each case. The CO<sub>2</sub> composition increases in the product stream after the liquefaction process, which is over 99% in all cases. Considering the delivery pressure in the three different capture method cases, the CO<sub>2</sub> composition is slightly higher when the delivery pressure is at 7 bar. This is because after the pressure drops to the delivery pressure at the valve, the composition of CO<sub>2</sub> is higher in the liquid phase, while in the vapour phase, the composition of impurities becomes higher and goes on another circle.

Fig. 5 presents the composition of different impurities in Cases 1-3. The composition of most impurities is lower after the liquefaction process in the product stream except CH<sub>3</sub>OH, H<sub>2</sub>S and SO<sub>2</sub> because the capability to remove CH<sub>3</sub>OH in the purge stream is insufficient so it will accumulate in each circle and the composition in the product stream is a little bit higher compared to the feed stream.

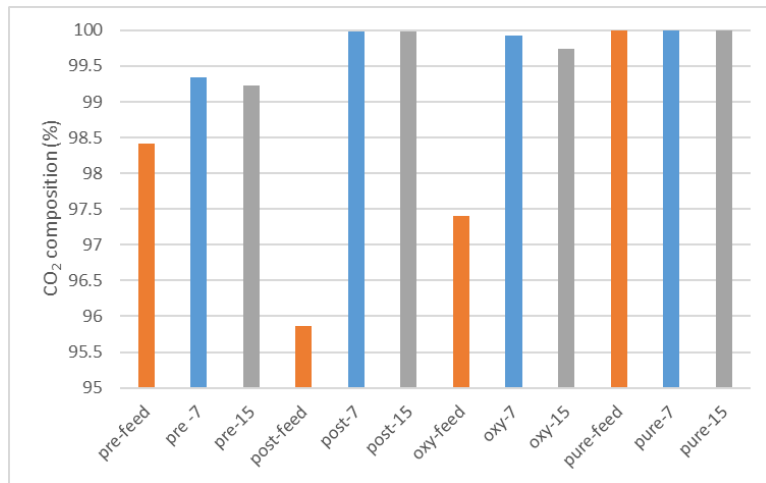


Fig. 4. CO<sub>2</sub> composition of the product stream in Cases 1 to 3 and Case 8. Orange column: feed stream; Blue column: product stream at 7 bar; Gray column: product stream at 15 bar.

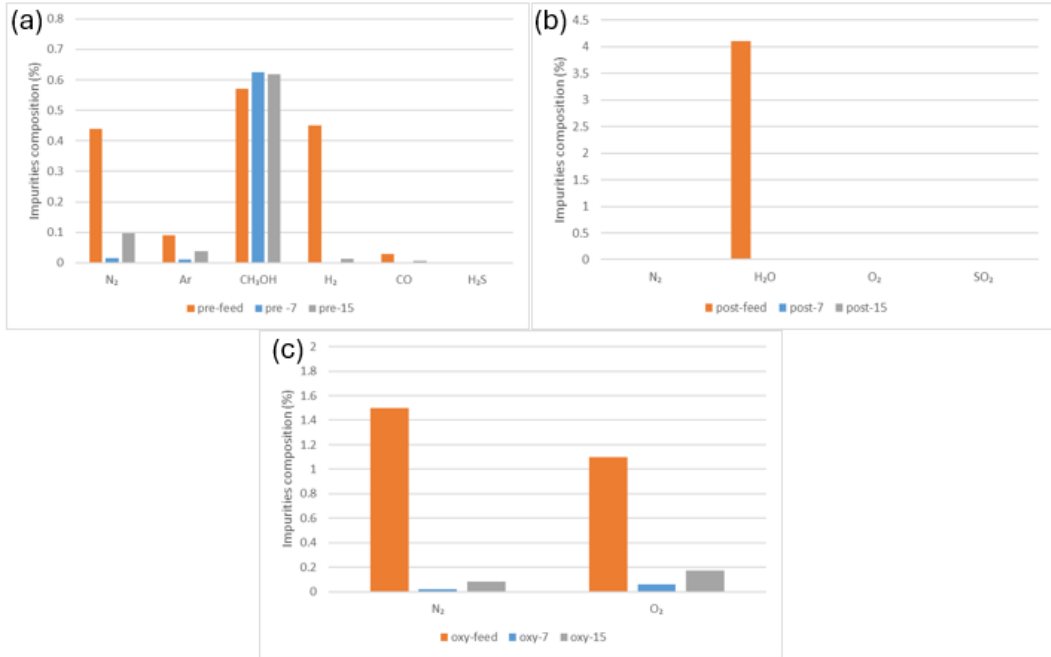


Fig. 5. Impurities composition of the feed streams and the product streams in (a) Case 1; (b) Case 2; (c) Case 3. Orange column: feed stream; Blue column: product stream at 7 bar; Gray column: product stream at 15 bar.

Similarly, the CO<sub>2</sub> product stream composition of cases 4 to 7 is shown in Table 3.2. In order to compare the difference in the composition of CO<sub>2</sub> and impurities between the feed stream and the product stream, the composition of the feed stream is added to Fig. 5 and Fig. 6 below.

Table 3.2. Composition of CO<sub>2</sub> production streams in Cases 4-7.

|                      | Cement-7 | Cement-15 | Iron-7 | Iron-15 | Power-7 | Power-15 | Refinery-7 | Refinery-15 |
|----------------------|----------|-----------|--------|---------|---------|----------|------------|-------------|
| CO <sub>2</sub> [%]  | 99.93    | 99.86     | 99.93  | 99.87   | 99.80   | 99.31    | 99.95      | 99.79       |
| N <sub>2</sub> [%]   | 0.03     | 0.11      | 0.04   | 0.09    | 0.01    | 0.03     | 0.05       | 0.21        |
| H <sub>2</sub> O [%] | 0.00     | 0.00      | 0.00   | 0.00    | 0.00    | 0.00     | 0.00       | 0.00        |
| O <sub>2</sub> [%]   | 0.02     | 0.03      | 0.03   | 0.04    | 0.19    | 0.66     | -          | -           |

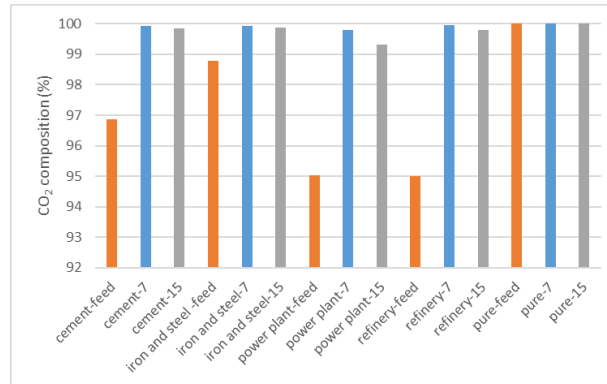


Fig. 6. CO<sub>2</sub> composition of the feed stream and the product stream in Cases 4-7. Orange column: feed stream; Blue column: product stream at 7 bar; Gray column: product stream at 15 bar.

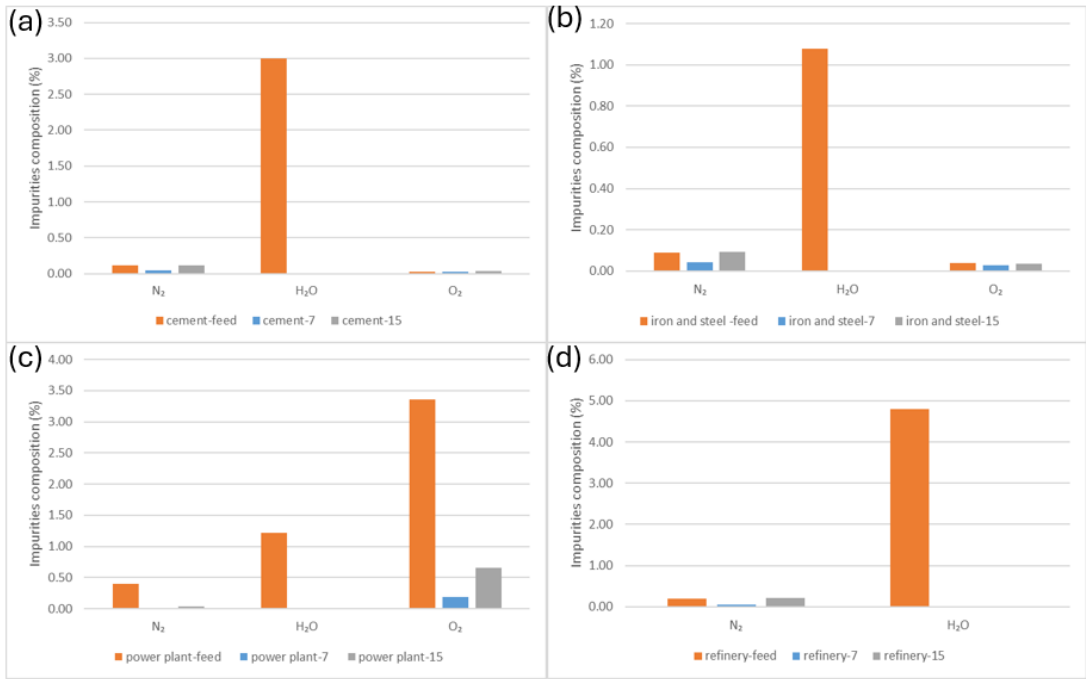


Fig. 7. Impurities composition of the feed stream and the product stream in (a) Case 4; (b) Case 5; (c) Case 6; (d) Case 7. Orange column: feed stream; Blue column: product stream at 7 bar; Gray column: product stream at 15 bar.

Fig. 6 shows the CO<sub>2</sub> composition in the product stream from 4 different industries. CO<sub>2</sub> composition increases after the liquefaction process in each case, reaching 99%.

The composition of impurities in the product stream from 4 different industries is presented in Fig. 7. The composition of water as an impurity drops obviously in every case, while the removal of some other impurities in some cases is not apparent because of the relatively low level of the impurities in the feed stream.

Given the requirement for impurities to be at very low levels for shipping, a purification process is essential to meet the shipping specifications. For instance, distillation effectively reduces most impurities.

### 3.2. Annual production of CO<sub>2</sub>

Since the composition of impurities is different, the mass flow rates of the purge stream are different and hence differ from each other. Moreover, the composition of the CO<sub>2</sub> in the product stream is different. The annual production of CO<sub>2</sub> in each case has some differences. It can be calculated from the mass flow rates of the CO<sub>2</sub> product stream and the composition of CO<sub>2</sub>.

The mass flow rates and annual production of CO<sub>2</sub> are shown in Table 3.3 below. The performances in terms of annual CO<sub>2</sub> production in the cement plant, iron and steel industry and refinery cases is very close to the results of the pure CO<sub>2</sub>, while Case 3, which chooses oxyfuel as the capture method, has the lowest annual CO<sub>2</sub> production. This is related to the composition of the CO<sub>2</sub> in the feed stream of each case because the flow rates of the feed stream in all cases are identical.

Table 3.3. The mass flow rates and annual production of CO<sub>2</sub> in all cases.

|             | Mass flow rates (kg/h) | Annual CO <sub>2</sub> production (Mt/yr) |
|-------------|------------------------|---|
| Pre-7       | 1.23×10 <sup>5</sup>   | 1.08                                      |
| Pre-15      | 1.24×10 <sup>5</sup>   | 1.09                                      |
| Post-7      | 1.32×10 <sup>5</sup>   | 1.16                                      |
| Post-15     | 1.32×10 <sup>5</sup>   | 1.16                                      |
| Oxy-7       | 1.03×10 <sup>5</sup>   | 0.91                                      |
| Oxy-15      | 1.05×10 <sup>5</sup>   | 0.92                                      |
| Cement-7    | 1.32×10 <sup>5</sup>   | 1.15                                      |
| Cement-15   | 1.33×10 <sup>5</sup>   | 1.16                                      |
| Iron-7      | 1.33×10 <sup>5</sup>   | 1.16                                      |
| Iron-15     | 1.34×10 <sup>5</sup>   | 1.17                                      |
| Power-7     | 1.04×10 <sup>5</sup>   | 0.91                                      |
| Power-15    | 1.07×10 <sup>5</sup>   | 0.94                                      |
| Refinery-7  | 1.30×10 <sup>5</sup>   | 1.14                                      |
| Refinery-15 | 1.31×10 <sup>5</sup>   | 1.15                                      |
| Pure-7      | 1.34×10 <sup>5</sup>   | 1.18                                      |
| Pure-15     | 1.34×10 <sup>5</sup>   | 1.18                                      |

### 3.3. Levelised cost

The CAPEX and OPEX for all 8 cases were obtained from the Aspen Process Economic Analyzer after simulations using Aspen Plus. The results and levelised cost are shown below in Table 3.4.

Table 3.4. CAPEX, OPEX and levelised cost in all Cases.

|             | CAPEX (M\$) | OPEX (M\$) | CO <sub>2</sub> production (Mt/yr) | levelised cost (\$/tCO <sub>2</sub> ) |
|-------------|-------------|------------|------------------------------------|---------------------------------------|
| Pre-7       | 33.32       | 17.57      | 1.08                               | 17.54                                 |
| Pre-15      | 30.72       | 16.52      | 1.09                               | 16.28                                 |
| Post-7      | 35.91       | 18.21      | 1.16                               | 16.33                                 |
| Post-15     | 34.17       | 17.52      | 1.16                               | 16.33                                 |
| Oxy-7       | 34.41       | 16.45      | 0.91                               | 19.70                                 |
| Oxy-15      | 33.87       | 15.91      | 0.92                               | 18.77                                 |
| Cement-7    | 36.82       | 18.32      | 1.16                               | 17.12                                 |
| Cement-15   | 35.68       | 17.33      | 1.16                               | 16.14                                 |
| Iron-7      | 36.32       | 18.86      | 1.17                               | 17.40                                 |
| Iron-15     | 36.08       | 17.91      | 1.17                               | 16.52                                 |
| Power-7     | 33.22       | 17.57      | 0.91                               | 20.72                                 |
| Power-15    | 32.71       | 16.87      | 0.94                               | 19.34                                 |
| Refinery-7  | 36.25       | 18.29      | 1.14                               | 17.29                                 |
| Refinery-15 | 35.10       | 17.06      | 1.15                               | 16.01                                 |
| Pure-7      | 37.73       | 17.84      | 1.18                               | 16.44                                 |
| Pure-15     | 34.41       | 16.67      | 1.18                               | 15.34                                 |

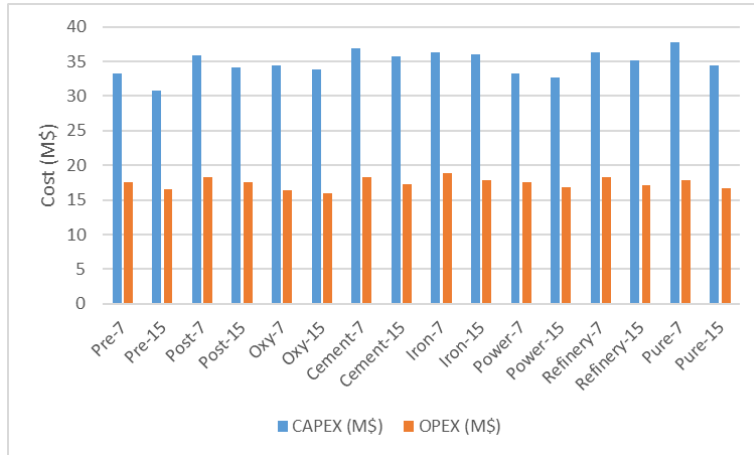


Fig. 8. CAPEX, OPEX in all Cases.

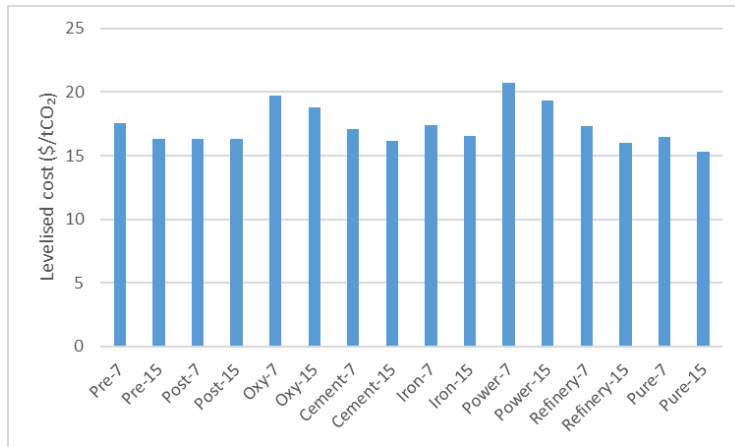


Fig. 9. Levelised cost in all Cases.

According to Table 3.4 and Fig. 8, Fig. 9, for all the cases, it is observed that the CAPEX values range from 30 to 38 million dollars per annum while the range of the OPEX values is from 15 to 19 million dollars per annum. Since the annual CO<sub>2</sub> production rate differs from case to case and from one delivery pressure to another, the CAPEX and OPEX cannot reflect the performance of the liquefaction process. The levelised cost, considered as a performance indicator, ranges from 15 to 21 dollars per ton of CO<sub>2</sub>. Pure CO<sub>2</sub> has the lowest annualized cost because of the high CO<sub>2</sub> production. For all the cases, comparison between different delivery pressures, the annualized cost at 15 bar is lower than at 7 bar in the liquefaction process, because more energy will be used to recompress the recirculated vapour from delivery pressure to the liquefaction pressure in the recirculation parts. The levelised cost of the post-combustion cases (\$16.33/tCO<sub>2</sub> at 7 bar and at 15 bar) are closer to the pure CO<sub>2</sub> case (\$16.44/tCO<sub>2</sub> at 7 bar and \$15.34/tCO<sub>2</sub> at 15 bar), which means the liquefaction performance of the post-combustion cases are the best in all the cases. Oxyfuel cases (\$19.70/tCO<sub>2</sub> at 7 bar and \$18.77/tCO<sub>2</sub> at 15 bar) and power plant cases (\$20.72/tCO<sub>2</sub> at 7 bar and \$19.34/tCO<sub>2</sub> at 15 bar) have relatively high levelised costs because of the relatively low production of CO<sub>2</sub> per year and the oxygen composition of the feed stream is relatively high in both cases.

## 4. Conclusions

The liquefaction process of feed streams with different compositions of CO<sub>2</sub> was simulated by Aspen Plus and analysed for CO<sub>2</sub> product composition, annual production of CO<sub>2</sub>, and levelised cost. Different levels and types of impurities have an impact on the performance of the liquefaction system.

For all selected cases, the CO<sub>2</sub> composition of the CO<sub>2</sub> production stream reaches 99%. Comparing delivery pressures of 7 bar and 15 bar, the CO<sub>2</sub> composition in the product stream is slightly higher at 7 bar, while the annual CO<sub>2</sub> production is greater at 15 bar. Additionally, both CAPEX and OPEX are lower at 15 bar, resulting in a reduced levelised cost and overall economic advantage at the higher delivery pressure. Excluding the pure CO<sub>2</sub> case, which is included for comparison, the refinery case at 15 bar achieves the lowest levelised cost (\$16.01/tCO<sub>2</sub>), while the power plant case at 7 bar has the highest (\$20.72/tCO<sub>2</sub>).

## Acknowledgements

Funded by the European Union under the Horizon Europe Framework Programme (Project name: CaLby2030; grant number: 101075416). Views and opinions expressed are, however, those of the authors only and do not necessarily reflect those of the European Union or the European Climate, Infrastructure and Environment Executive Agency (CINEA). Neither the European Union nor the granting authority can be held responsible for them. The project is also supported by the UK Research and Innovation (UKRI).

## References

- [1] IEA. (2022). Energy and CO<sub>2</sub> Status Report.
- [2] The Paris Agreement. (2015). Retrieved from United Nations: <https://www.un.org/en/climatechange/paris-agreement>.
- [3] Allen, M., Dube, O. P., Solecki, W., Aragón-Durand, F., Cramer, W., Humphreys, S., & Kainuma, M. (2018). Special Report: Global Warming of 1.5 C. Intergovernmental Panel on Climate Change (IPCC).
- [4] Yadav, S., & Mondal, S. S. (2022). A review on the progress and prospects of oxy-fuel carbon capture and sequestration (CCS) technology. *Fuel*, 308, 122057.
- [5] Ahmed, A. S., Rahman, M. R., & Bakri, M. K. (2021). A Review Based on Low-and High-Stream Global Carbon Capture and Storage (CCS) Technology and Implementation Strategy. *Journal of Applied Science & Process Engineering*, 8(1), 722-737.
- [6] Jakobsen, J., Roussanaly, S., & Anantharaman, R. (2017). A techno-economic case study of CO<sub>2</sub> capture, transport and storage chain from a cement plant in Norway. *Journal of cleaner production*, 144, 523-539.
- [7] Tangen, G., Kim, I., Brunsvold, A., Mølnvik, M., Vævelstad, S., Skurtveit, E., . . . Eliasson, P. (2021). Impact of Innovations from the Norwegian CCS Research Centre (NCCS). TCCS-11. CO<sub>2</sub> Capture, Transport and Storage. Trondheim 22nd–23rd June 2021. Short Papers from the 11th International Trondheim CCS Conference. SINTEF Academic Press.
- [8] Neele, F., Koenen, M., van Deurzen, J., Seebregts, A., Groenewegen, H., & Thielemann, T. (2011). Large-scale CCS transport and storage networks in North-west and Central Europe. *Energy Procedia*, 4, 2740-2747.
- [9] Mualim, A., Juwari, Altway, A., & Renanto. (2023). Systematic Framework for CO<sub>2</sub> Transport Design of CCS System in the Archipelagic State. *Process Integration and Optimization for Sustainability*, 7(1-2), 269-292.
- [10] Bhattacharyya, D., Turton, R., & Zitney, S. E. (2017). Acid gas removal from syngas in IGCC plants. In *Integrated Gasification Combined Cycle (IGCC) Technologies* (pp. 385-418). Woodhead Publishing.
- [11] Magli, F., Spinelli, M., Fantini, M., Romano, M. C., & Gatti, M. (2022). Techno-economic optimization and off-design analysis of CO<sub>2</sub> purification units for cement plants with oxyfuel-based CO<sub>2</sub> capture. *International Journal of Greenhouse Gas Control*, 115, 103591.
- [12] De Visser, E., Hendriks, C., Barrio, M., Mølnvik, M. J., de Koeijer, G., Liljemark, S., & Le Gallo, Y. (2008). Dynamis CO<sub>2</sub> quality recommendations. *International journal of greenhouse gas control*, 2(4), 478-484.
- [13] Posch, S., & Haider, M. (2012). Optimization of CO<sub>2</sub> compression and purification units (CO2CPU) for CCS power plants. *Fuel*, 101, 254-261.
- [14] Wetenhall, B., Aghajani, H., Chalmers, H., Benson, S., Ferrari, M., Li, J., . . . Davison, J. (2014). Impact of CO<sub>2</sub> impurity on CO<sub>2</sub> compression, liquefaction and transportation. *Energy Procedia*, 63, 2764-2778.
- [15] Zeng, Y., Luo, J., Li, K., & Arafat, M. (2018). Impacts of Impurities on Corrosion of Supercritical CO<sub>2</sub> Transportation Pipeline Steels. In *NACE CORROSION* (pp. NACE-2018). NACE.
- [16] Xiang, Y., Xu, M., & Choi, Y. S. (2017). State-of-the-art overview of pipeline steel corrosion in impure dense CO<sub>2</sub> for CCS transportation: Mechanisms and models. *Corrosion Engineering, Science and Technology*, 52(7), 485-509.

- [17] Roussanaly, S., Vitvarova, M., Anantharaman, R., Berstad, D., Hagen, B., Jakobsen, J., ... & Skaugen, G. (2020). Techno-economic comparison of three technologies for pre-combustion CO<sub>2</sub> capture from a lignite-fired IGCC. *Frontiers of Chemical Science and Engineering*, 14(3), 436-452.
- [18] Sanpasertparnich, T., Idem, R., Bolea, I., deMontigny, D., & Tontiwachwuthikul, P. (2010). Integration of post-combustion capture and storage into a pulverized coal-fired power plant. *International Journal of Greenhouse Gas Control*, 4(3), 499-510.
- [19] White, V., Wright, A., Tappe, S., & Yan, J. (2013). The air products Vattenfall oxyfuel CO<sub>2</sub> compression and purification pilot plant at Schwarze Pumpe. *Energy Procedia*, 37, 1490-1499.
- [20] Voldsgaard, M., Gardarsdottir, S., De, L. E., Pérez-Calvo, J., Jamali, A., Berstad, D., ... Jordal, K. (2019). Comparison of technologies for CO<sub>2</sub> capture from cement production—Part 1: Technical evaluation. *Energies*, 12(3), 559.
- [21] Luca, A. V., & Petrescu, L. (2021). Membrane technology applied to steel production: Investigation based on process modelling and environmental tools. *Journal of Cleaner Production*, 294, 126256.
- [22] He, X., Chen, D., Liang, Z., & Yang, F. (2022). Insight and comparison of energy-efficient membrane processes for CO<sub>2</sub> capture from flue gases in power plant and energy-intensive industry. *Carbon Capture Science & Technology*, 2, 100020.
- [23] Madugula, A. C., Sachde, D., Hovorka, S. D., Meckel, T. A., & Benson, T. J. (2021). Estimation of CO<sub>2</sub> emissions from petroleum refineries based on the total operable capacity for carbon capture applications. *Chemical Engineering Journal Advances*, 8, 100162